Pergamon

Int. J. Heat Mass Transfer. Vol. 39, No. 13, pp. 2625–2639, 1996

0017-9310/96 $15.00+0.00

0017-9310(95)00373-8

Forced convection in-tube steam condensation in the presence of noncondensable gases

H. A. HASANEIN, M. S. KAZIMI† and M. W. GOLAY

Nuclear Engineering Department, Massachusetts Institute of Technology, Cambridge, MA 02139, U.S.A.

(*Received* 24 *January* 1995 *and in final form* 21 *October* 1995)

Abstract—An experimental and analytical investigation has been conducted to determine the effects of the presence of noncondensable gases on in-tube steam condensation under forced convection conditions. The local mixture Nusselt numbers were correlated in terms of the local mixture Reynolds number, mixture Jakob number, and the gas mass fractions or the mixture Schmidt number. Correlations including the mixture Schmidt number did better in representing the condensation process in the presence of one noncondensable gas. The experiments covered steam/gas mixture inlet Reynolds numbers from about 6000 to 26 000, inlet helium mass fraction range from 0.022 up to 0.20, inlet air mass fraction range from 0.045 up to 0.20, and mixture inlet temperature of 100°C and 130°C (corresponding to a pressure range from 114 to 603 kPa). The ratios of the condensate film thermal resistance to the thermal resistance of the steam/noncondensable gas mixture at the same bulk temperature were calculated. In general, the condensate film thermal resistance was found to be significant for turbulent gas mixture conditions ($Re > 6000$) and relatively low gas mass fraction ($W < 0.2$). A diffusion-based, simplified boundary layer model has been developed. The steady-state radial diffusion equations of the mixture components were solved in order to obtain the steam mass flux at the interface between the condensate film and the mixture. The effect of the axial flow was included in terms of an effective boundary layer thickness which decreases with mixture Reynolds number. The model included the effect of more than one noncondensable gas on steam condensation. The model-predicted mixture heat transfer coefficients were favorably compared to the experimental results. Copyright © 1996 Elsevier Science Ltd.

1. INTRODUCTION

The presence of noncondensables in steam greatly inhibits the condensation process. This inhibitive effect is a major concern in the design of much condensing equipment in the chemical process industry where in-tube condensation is employed (e.g. evaporation, distillation and crystallization processes). In the nuclear industry the effect of noncondensable gases on steam condensation is one of the major safety-related issues. In a nuclear containment building, air and the accidental presence of hydrogen represent the main noncondensable gases. While air exists naturally in the containment building, hydrogen can exist in the case of a loss of coolant accident (LOCA) or steam line break accident. The principal sources for hydrogen are the exothermic fuel cladding chemical reaction with steam, the radiolytic decomposition of water and the corrosion of certain metallic species present in the containment. Thus for safety analysis, mixtures of steam, air and hydrogen may be assumed present in the containment. Experimental assessments of the effects of air, hydrogen and the simultaneous effects of air and hydrogen on steam condensation are therefore needed.

Many experimental and theoretical efforts have addressed the effects of noncondensables on condensation. Jensen [1] offers interesting discussions on the progress made up to 1988. However, most of the investigations focused on the determination of the average values of condensation heat transfer coefficients. Recently, a number of studies investigated the effects of noncondensables on the local values of the condensation heat transfer coefficients. Vierow [2] performed experiments to investigate the effects of air on local steam condensation in natural circulation in a vertical tube. Dehbi [3] performed steam/air and steam/air/helium experiments for external condensation on a vertical wall under turbulent natural conditions. It is a common practice in experiments studying the effects of hydrogen on condensations that hydrogen is replaced by helium because of the more demanding handling of hydrogen due to its explosive potential above a certain concentration. Both helium and hydrogen are light gases and have similar thermal and diffusive characteristics. Ogg [4] ran air/steam and helium/steam experiments in a vertical tube under forced flow conditions. Siddique [5] performed steam/air and steam/helium experiments in a vertical tube under forced flow conditions. However, the range of the steam/helium mixture Reynolds number and that of helium mass fraction were limited. There are no known experiments in the literature on the simultaneous effects of air and helium on steam condensation under forced flow conditions.

† Author to whom correspondence should be addressed.

NOMENCLATURE

A	tube inside surface area, or system parameter [see equation (7)]
C_p	specific heat capacity at constant pressure
D	diffusion coefficient
D_{12}	binary diffusion coefficient
d	condensing tube inner diameter (ID)
g	acceleration of gravity
h	condensation heat transfer coefficient
h_{fg}	latent heat of condensation
Ja	Jakob number
k	thermal conductivity
l_o	effective tube length
M	molecular mass
m	mass flow rate
m''	mass flux
Nu	Nusselt number
P	pressure
Pr	Prandtl number
Q	volumetric flow rate
q''	heat flux
Re	Reynolds number
Sc	Schmidt number
T	temperature
W	mass fraction
Y	mole fraction.

Greek symbols

δ	condensate film thickness
μ	dynamic viscosity
ν	kinematic viscosity
ρ	density.

Subscripts and Superscripts

a	air
b	bulk
Ch	based on Chen correlation [see equation (6)]
c	coolant in the annulus
con	condensate film
f	liquid film, condensate
g	saturation vapor
h	helium
i	interface
in	condenser inlet
κ	value at node K
l	saturation liquid
mix	steam/noncondensable gas mixture
N	based on Nusselt assumption [see equation (5)]
nc	noncondensable gas
r	reference
sat	saturation
v	steam
w	tube inside wall.

In general, there exists two main methods for analyzing the forced convective condensation of steam in the presence of noncondensables. The first is the boundary layer (BL) based models which employ similarity solutions, integral methods and finite difference techniques [6–15]. The second one is the heat and mass transfer (HMT) analogy based models. Colburn and Hougen [16] were the first to develop a stepwise iterative solution method for predicting the condensation heat transfer rate from a vapor/noncondensable mixture based on the heat and mass transfer analogy. Since then, a number of researchers [17–23] have proposed approximate numerical analyses to simplify and improve the Colburn and Hougen methodology which is practically cumbersome. However, the above mentioned approximate methods dealt with only one noncondensable gas in the steam/gas mixture.

The objective of the present investigation is to measure the local heat transfer coefficients of condensing steam in the presence of helium and the simultaneous presence of air and helium in vertical tubes under forced convection conditions, and to provide evaluation models of condensation Nusselt numbers under such circumstances.

2. EXPERIMENTAL SET-UP AND DATA ANALYSIS

2.1. *Description of the apparatus*

Figure 1 shows the flow diagram of the experimental test facility used in the work reported here. It consisted of an open cooling water circuit and an open steam/noncondensable gas flow path. The test section used a stainless steel tube for condensation of the mixture on its inner surface. The dimensions of the tube were 50.8 mm outside diameter (OD), 46.0 mm inside diameter (ID) and 2.54 m in length. The stainless steel (SS) tube was also surrounded by a 62.7 mm (ID) jacket pipe. Four immersion type sheathed electrical heaters that can be individually controlled (on or off) and which are rated at 7.0 kW each were used to generate steam by boiling water in a cylindrical stainless steel vessel of 5.0 m height and 0.45 m inside diameter. Finer control of the power level was achieved by means of a Variac connected to one of the heaters. A pressure regulating valve, a flow control valve and a calibrated rotameter were used to supply compressed gas to the base of the steam generating vessel. The vessel was also used as a mixing chamber where gas was injected near the vessel bottom to

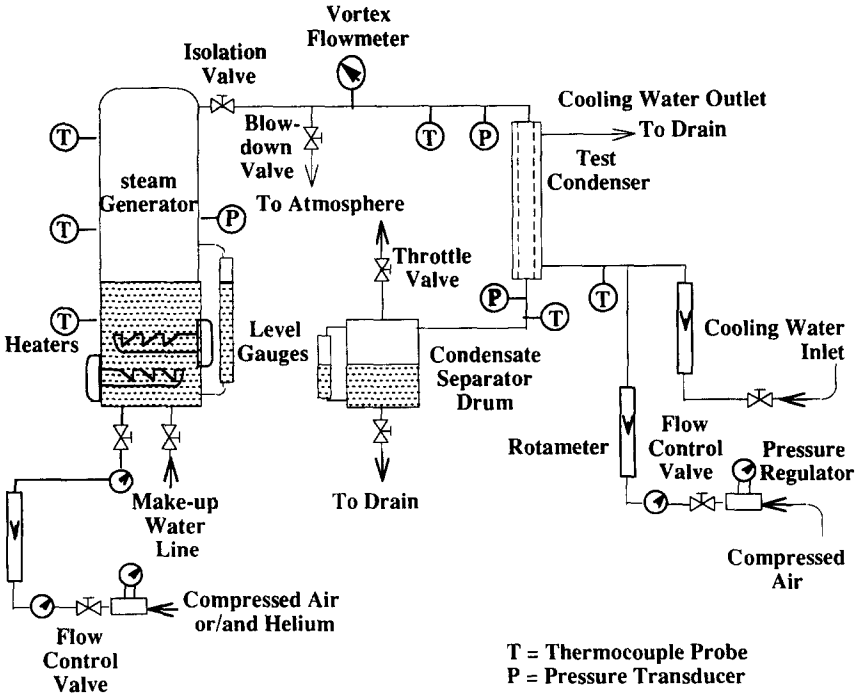

Fig. 1. Schematic of experimental facility.

ensure mixing with the steam and formation of a homogeneous gas mixture in thermal equilibrium. The steam/noncondensable gas mixture left the pressure vessel through an isolation valve which was fitted to the side, near the top of the vessel. Figure 2 depicts the thermocouple locations of the cooling water, the inside and outside of the tube wall, and the condenser tube centerline gases. However, most of the outer wall thermocouples were not functional. Replacing these thermocouples was not possible because of the nature of the design. This situation rendered the service of the outer wall thermocouples useless. J-type (iron-constantan) thermocouples were used for all temperature measurements.

Since the coolant flow rate was kept so low that the flow was laminar in most cases, small amounts of air were bubbled into the cooling water flow in order to enhance turbulence and mixing. Based on the conclusions of an investigation [24] on the effects of the cooling conditions on the determination of the local heat fluxes, and consequently local condensation heat transfer coefficients, a full scale visualization experimental facility was built in order to simulate the coolant annulus of the actual test section and determine the amount of air which is sufficient for good mixing [25].

A data acquisition (DA) system with 40 input channels was used to collect data from the thermocouples, pressure transducers and vortex flow meter. The DA system was comprised of a scanner and a data processor linked to a personnel computer. The scanner scanned at a rate of 40 channels per s and the processor was adjusted to record data every minute and to perform average and standard deviation calculations. At steady-state the input readings stabilized, as was manifested by low data standard deviation values.

The test facility and experimental procedure are described in details in ref. [25].

2.2. *Data analysis and experimental errors*

The local values of the heat fluxes were calculated from the following equation obtained from a steady-state energy balance on the coolant side:

$$q''(x) = \frac{m_c C_{p,c}}{\pi d} \frac{dT_c(x)}{dx} \tag{1}$$

with the local gradients of the cooling water temperature profile $dT_c(x)/dx$ being determined using a least squares polynomial fit of the cooling water temperature profile. The adjusted R^2 value for the fit of the data to the polynomial was greater than 0.98 so that the error associated with the curve fittings was small. Then, the local heat transfer coefficients were calculated using the following equations:

$$h(x) = \frac{q''(x)}{T_{sat}(x) - T_w(x)} \tag{2}$$

where $T_{sat}(x)$ is the saturation temperature corresponding to the vapor pressure and $T_w(x)$ is the condensing tube inner wall temperature at the axial position x of the condensing tube. The local condensate film flow rate was determined from the following equation:

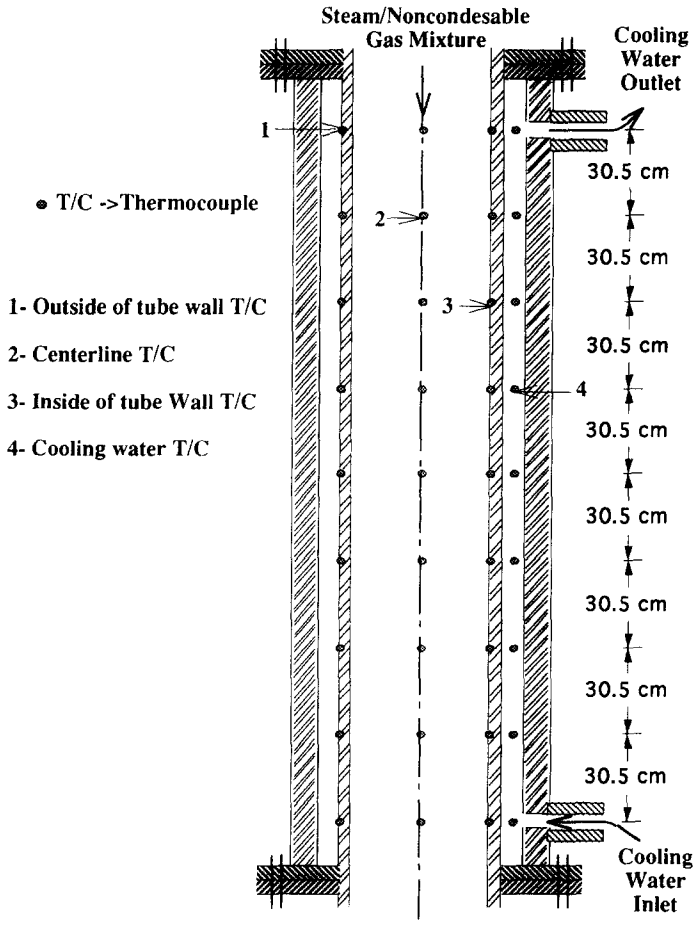

Fig. 2. Thermocouple locations.

$$m_{\mathrm{con}}(x) = \pi d \int_0^x \frac{q_i''(x')}{h_{\mathrm{fg}}(x')}\,\mathrm{d}x' \tag{3}$$

where h_{fg} is evaluated at the saturation temperature T_{sat}. The local condensate film Reynolds number was then calculated from the following equation:

$$Re_{\mathrm{f}}(x) = \frac{4m_{\mathrm{con}}(x)}{\pi d\mu_{\mathrm{f}}(x)} \tag{4}$$

where μ_{f} is the condensate film dynamic viscosity evaluated at $T_{\mathrm{r}} = T_{\mathrm{w}} + 0.33(T_{\mathrm{sat}} - T_{\mathrm{w}})$ and d is the condensing tube inside diameter. The local condensation heat transfer coefficients of the condensate film $h_{\mathrm{f}}^{\mathrm{N}}$, according to the Nusselt theory [26] for laminar film behavior can be calculated using the following expression [27]:

$$Nu_{\mathrm{f}}^{\mathrm{N}}(x) = \frac{h_{\mathrm{f}}^{\mathrm{N}}(x)}{k_{\mathrm{l}}(x)}\left(\frac{v_{\mathrm{l}}^2(x)}{g}\right)^{1/3} = \left(\tfrac{3}{4}Re_{\mathrm{f}}(x)\right)^{1/3} \tag{5}$$

where $Nu_{\mathrm{f}}^{\mathrm{N}}$ is the condensate film Nusselt number based on Nusselt theory, v_{l} is the condensate film kinematic viscosity, and k_{l} is the condensation film thermal conductivity at T_{r}. However, Nusselt theory assumes negligible drag by vapor, negligible effect of condensate film acceleration and heat convection. Employing these assumptions should yield conservative (i.e. underestimated) values of pure steam Nusselt numbers. Therefore, for a realistic evaluation of pure steam Nusselt numbers, the local condensation heat transfer coefficients of the condensate film $h_{\mathrm{f}}^{\mathrm{Ch}}$ based on a correlation developed by Chen *et al.* [28] are also calculated. This correlation incorporates the effects of interfacial shear stress, interfacial waviness, and turbulent transport in the condensate film and is expressed as:

$$Nu_{\mathrm{f}}^{\mathrm{Ch}}(x) = \frac{h_{\mathrm{f}}^{\mathrm{Ch}}(x)}{k_{\mathrm{l}}(x)}\left(\frac{v_{\mathrm{l}}^2(x)}{g}\right)^{1/3} = \left[\left(0.31Re_{\mathrm{f}}^{-1.32} + \frac{Re_{\mathrm{f}}^{2.4}Pr_{\mathrm{f}}^{3.9}}{2.37\times 10^{14}}\right)^{1/3} + \frac{Pr_{\mathrm{f}}^{1.3}A}{771.6}(Re_{\mathrm{T}} - Re_{\mathrm{f}})^{1.4}Re_{\mathrm{f}}^{0.4}\right]^{1/2} \tag{6}$$

where A is given by

$$A = \frac{0.252\mu_{\mathrm{l}}^{1.177}\mu_{\mathrm{g}}^{0.156}}{d^2 g^{2/3}\rho_{\mathrm{l}}^{0.553}\rho_{\mathrm{g}}^{0.78}}. \tag{7}$$

In equations (6) and (7), Re_f is the local condensate film Reynolds number, Re_T represents the film Reynolds number of the condensate if total condensation of the steam takes place and A is a system parameter which accounts for the gravitational and viscous forces. The local steam mass flow rate, the local steam/noncondensables mixture flow rate, and the local bulk steam mass fraction in the mixture are calculated from the following equations:

$$m_v(x) = m_v^{in}(x) - m_{con}(x) \tag{8}$$

$$m_{mix}(x) = m_v(x) + \sum_i^n m_i^{nc} \tag{9}$$

and

$$W_i^{nc}(x) = \frac{m_i^{nc}}{m_{mix}(x)} \tag{10}$$

where $m_s^{in}(x)$ is the inlet steam mass flow rate and m_i^{nc} is the mass flow rate of the ith component of the noncondensable gas in the mixture. The local steam/gas mixture Reynolds mixture is obtained from

$$Re(x) = \frac{4m_{mix}}{\pi d \mu_{mix}} \tag{11}$$

where μ_{mix} is the steam/noncondensables mixture dynamic viscosity. The local steam/noncondensables mixture experimental Nusselt number is obtained from

$$Nu(x) = \frac{h(x)d}{k_{mix}} \tag{12}$$

where k_{mix} is the steam/gas mixture thermal conductivity. The steam/gas mixture Schmidt number is determined from

$$Sc(x) = \frac{\mu_{mix}}{\rho_{mix} D_v} \tag{13}$$

where ρ_{mix} is the mixture density and D_v is the mass diffusion coefficient of the vapor in the noncondensable gases. A discussion of the diffusion coefficient D_v will be presented later in Section 5.2. The mixture Jakob number is given by

$$Ja(x) = \frac{C_{p,mix}(T_{sat}(x) - T_i(x))}{h_{fg}} \tag{14}$$

where $C_{p,mix}$ is the steam/gas mixture specific heat capacity and h_{fg} is the latent heat of condensation. The individual properties are evaluated from ref. [29] and the mixture properties were evaluated at the bulk temperature and following the procedure explained in refs. [12, 30]. The maximum uncertainty in determining the condensation heat transfer coefficient was $\pm 30.5\%$ as shown in ref. [25].

3. RESULTS AND DISCUSSION

Condensation in steam/helium systems and steam/air/helium systems has been experimentally investigated over a wide range of system parameters. The steam/helium experiments covered steam/helium mixture inlet Reynolds number from about 6000 to about 24 000, inlet helium mass fractions from 0.022 up to 0.20, and mixture inlet temperatures of 100 and 130°C. The steam/air/helium experiments covered steam/air/helium mixture inlet Reynolds numbers from about 6500 to 26 500, inlet helium mass fractions from 0.023 up to 0.20, inlet air mass fractions from 0.045 up to 0.20 and mixture inlet temperatures of 100 and 130°C. The corresponding pressure range was between 114 to 603 kPa. Complete sets of reduced data are given in ref. [25].

3.1. *Results of steam/helium mixture experiments*

Figure 3 shows profiles of the experimental heat transfer coefficients of steam in the presence of helium, helium mass fraction, mixture Schmidt number and mixture Jakob number. The figure shows the gradual decrease of the experimental heat transfer coefficients as helium mass fraction, mixture Schmidt number and mixture Jakob number increase. Figure 4 shows profiles of the experimental heat transfer coefficients of steam in the presence of helium, the calculated heat transfer coefficients of pure steam using Nusselt assumptions [26], and the calculated heat transfer coefficients of pure steam using the correlation of Chen *et al.* [28]. The figure shows the gradual decrease of the experimental heat transfer coefficients as the mixture Reynolds numbers decrease. It also shows that the calculated pure steam or film heat transfer coefficients are higher than those of steam/helium mixtures. The heat transfer coefficients of pure steam evaluated using the Nusselt assumptions are lower than those evaluated using the correlation of Chen *et al.*; a result which is expected, since the effects of waviness and vapor shear should increase the condensate film heat transfer coefficients. It should be noted that the increase of the condensation heat transfer coefficients in the mid height of the test condenser is due to the condenser wall temperature inversion at this location. Attempts have been made to explain this temperature inversion as described in ref. [25], but no satisfactory answer was given. However, since the cause of this temperature inversion is still unknown, the data point corresponding to this inversion was not included in the data correlations. The experimental mixture condensation heat transfer coefficient (or Nusselt number, Nu) was then correlated in terms of helium bulk mass (mole) fraction W_h (Y_h), mixture Jakob number Ja, mixture Reynolds number Re, and mixture Schmidt number Sc. However, since the mixture Schmidt number implicitly includes the effect of the helium mass (mole) fraction on steam condensation, including both parameters in one correlation was avoided in order not to duplicate the effects.

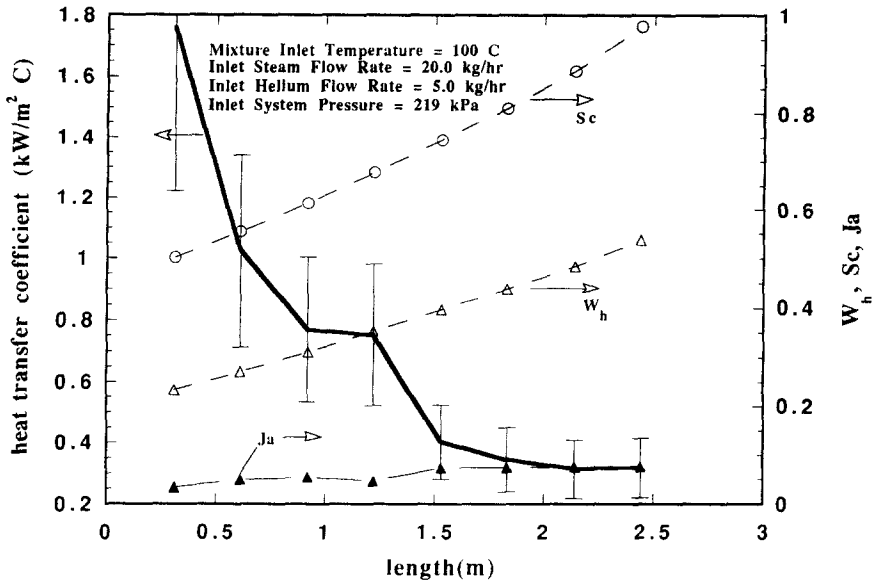

Fig. 3. Heat transfer coefficient variations with helium mass fraction, mixture Schmidt number and mixture Jakob number along the condensing tube length.

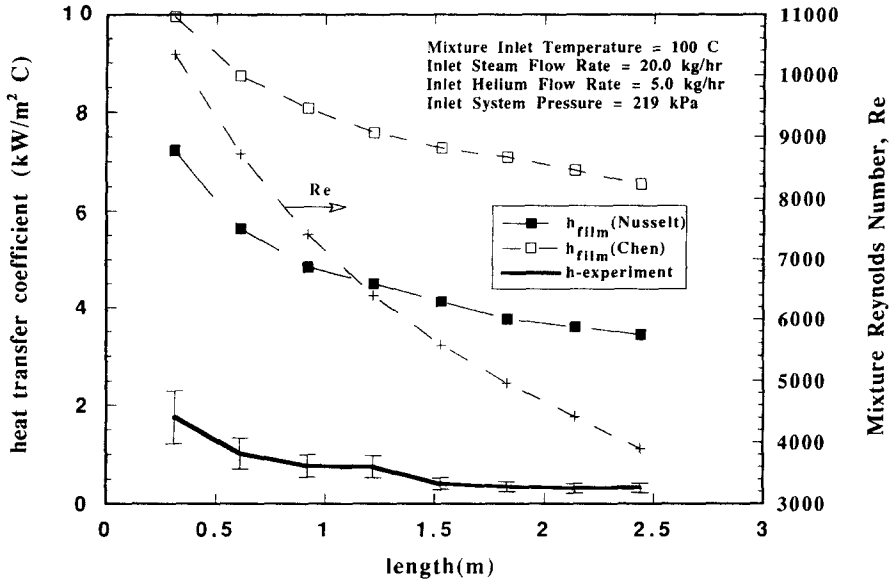

Fig. 4. Heat transfer coefficients variations with mixture Reynolds number along the condensing tube length.

Therefore, the steam/helium experimental data were calculated by relationships of the forms

$$Nu = \text{const} \cdot Re^{a} W_h^{b} Ja^{c} \tag{15}$$

and

$$Nu = \text{const} \cdot Re^{g} Sc^{h} Ja^{i}. \tag{16}$$

The above expressions were linearized using logarithmic transformation, and then a multiple regression analysis was performed in order to obtain the values of the coefficients. The result was the following correlations:

$$Nu = 1.279 Re^{0.256} W_h^{-0.741} Ja^{-0.952} \tag{17}$$

and

$$Nu = 2.244 Re^{0.161} Sc^{-1.652} Ja^{-1.038}. \tag{18}$$

The mixture Schmidt number represents the momentum to diffusive characteristics of the mixture and also includes the effects of helium mass (mole) fraction. This explains the better fitting to equation (18) of the experimental data [25]. Figure 5 shows a comparison between equation (18) and the experimental data. However, it should be noted that equa-

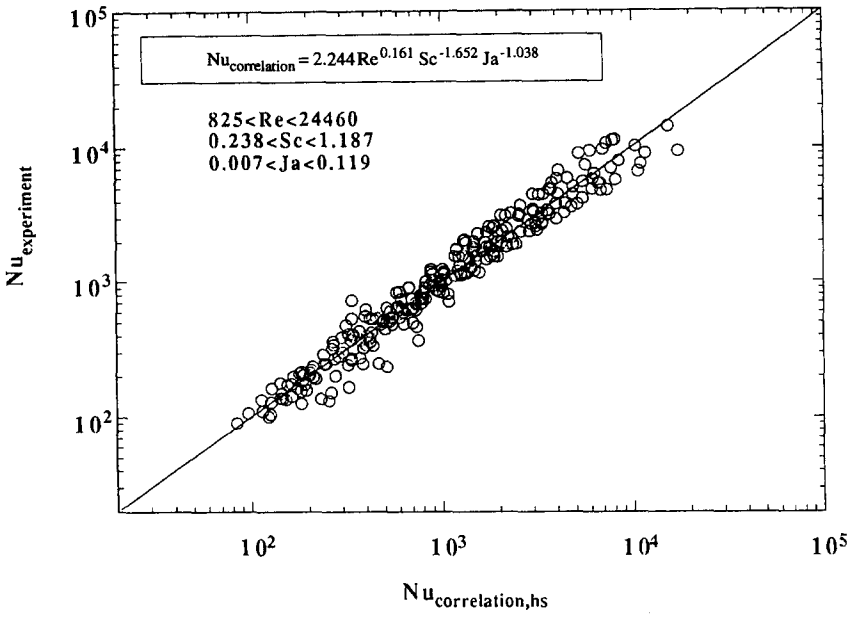

Fig. 5. Comparison between the experimentally obtained Nusselt numbers and those obtained by steam/helium correlation, equation (18).

tions (17) and (18) were obtained from a set of data that reach a higher value of Re (24 000) than shown in the figure.

Comparison with steam/helium correlation of Siddique et al. [5]. Siddique *et al.* [5] performed steam/helium condensation experiments and recommended the following correlation:

$$Nu = 0.537 Re^{0.433} W_h^{-1.249} Ja^{-0.624} \quad (19)$$

within the range,

$$0.02 < W_h < 0.52$$

$$300 < Re < 11\,400$$

and

$$0.004 < Ja < 0.07.$$

Within the above range of parameters, the experimental steam/helium heat transfer coefficients were plotted against those obtained from equation (19) as shown in Fig. 6. The plot shows good agreement between the predicted heat transfer coefficients using the Siddique–Golay–Kazimi's correlation and the experimentally obtained ones.

3.2. *Results of steam/air/helium mixture experiments*

It was found that the experimental mixture condensation heat transfer coefficient (or Nusselt number, Nu) decreased with helium bulk mass (mole) fraction $W_h(Y_h)$, air bulk mass (mole) fraction $W_a(Y_a)$, mixture Jakob number Ja, and with mixture Schmidt number Sc, while it increased with steam/air/helium mixture Reynolds number. The experimental data was then correlated in terms of these parameters in a way similar to that used in Section 3.1. The result was the following correlations:

$$Nu = 0.12 Re^{0.368} W_a^{-0.554} W_h^{-0.676} Ja^{-0.931} \quad (20)$$

and

$$Nu = 0.199 Re^{0.327} Sc^{-2.715} Ja^{-1.058}. \quad (21)$$

Figure 7 shows comparisons between the condensation Nusselt numbers obtained using the last correlation and the experimentally obtained Nusselt numbers. Again, this correlation, equation (21), included mixture Schmidt number and provided a good fit with the experimental data for the same reasons mentioned in the previous section. Another correlation was also obtained which applies to helium and steam mixtures with or without air in the mixture. This correlation used the steam/helium correlation, equation (18) as its basis in correlating the steam/air/helium experimental data. The result was the following correlation:

$$Nu = 1.279 Re^{0.256} (1 - 1.681 W_a) W_h^{-0.741} Ja^{-0.952}. \quad (22)$$

A comparison between the condensation Nusselt numbers obtained using the above correlation, equation (22) and the experimentally obtained Nusselt numbers is shown in Fig. (8).

4. PERFORMANCE MODEL

The following steps outline a procedure by which the correlations developed in the previous section are to be used in practice in sizing a vertical condensing

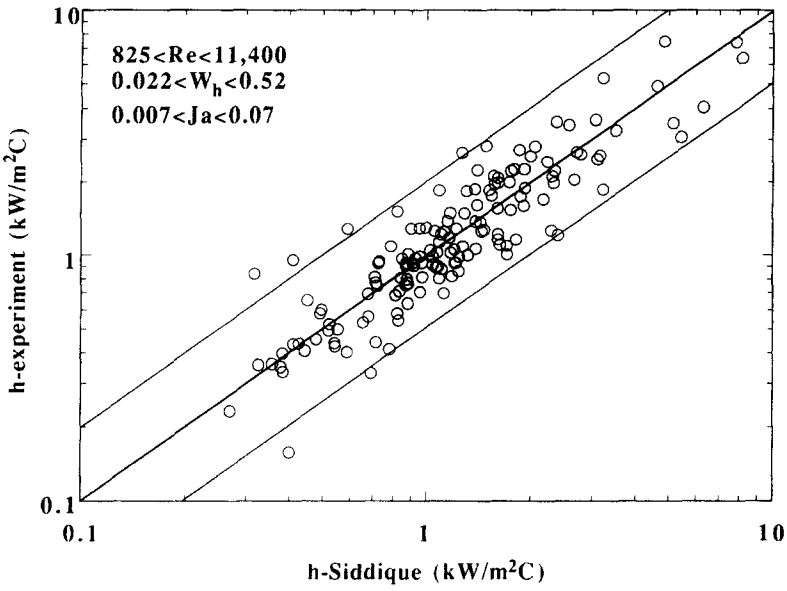

Fig. 6. Comparison between the experimental condensation heat transfer coefficients and those obtained using a correlation produced by Siddique *et al.*, equation (19).

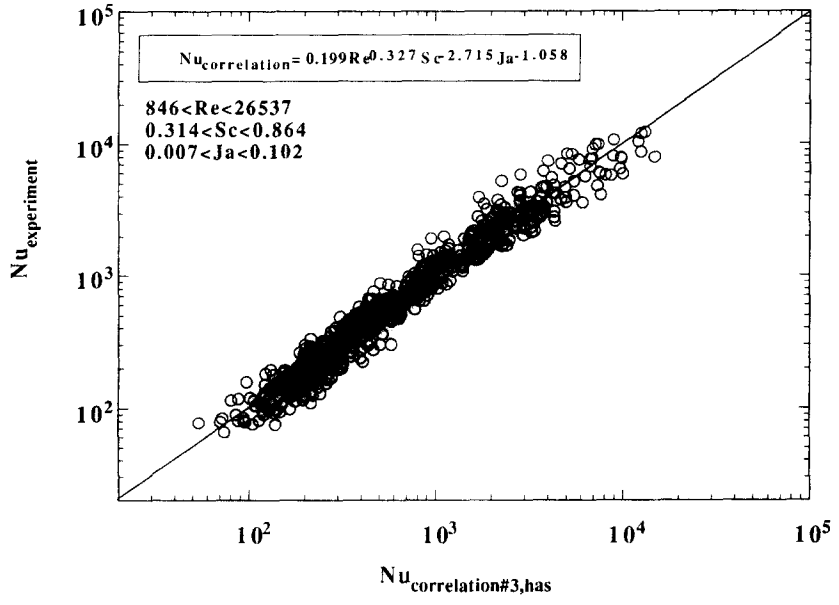

Fig. 7. Comparison between the experimentally obtained Nusselt numbers and those obtained by steam/air/helium correlation, equation (21).

tube in which a mixture of steam and noncondensable gases flows downward. In this model the temperature profile of the condenser wall as well as the conditions at its inlet are assumed to be known. The inlet conditions are the system total pressure, mixture bulk temperature, mass fractions of the noncondensable gases, steam flow rate, and the flow rates of the noncondensable gases:

(1) At one step ΔT_b of the steam/gas mixture bulk temperature down the condenser length, l, the new bulk temperature $T_b^{(\kappa+1)}$ is given by

$$T_b^{(\kappa+1)} = T_b^{(\kappa)} - \Delta T_b. \tag{23}$$

Assuming the mixture components are in thermodynamic equilibrium with one another, the vapor pressure $P_v^{(\kappa+1)}$ corresponding to this new bulk temperature is calculated from

$$P_{v,b}^{(\kappa+1)} = P_{sat}\{T_b^{(\kappa+1)}\}. \tag{24}$$

Since the total system pressure P_t is almost constant along the condensing tube, $W_{v,b}^{(\kappa+1)}$, $W_{a,b}^{(\kappa+1)}$, and $W_{h,b}^{(\kappa+1)}$ can be obtained by solving the system of equations (51)–(54) at $T_b^{(\kappa+1)}$. The system of equations (48)–(51) will be presented later in Section 5.2.

(2) Since the noncondensable gases mass flow rates

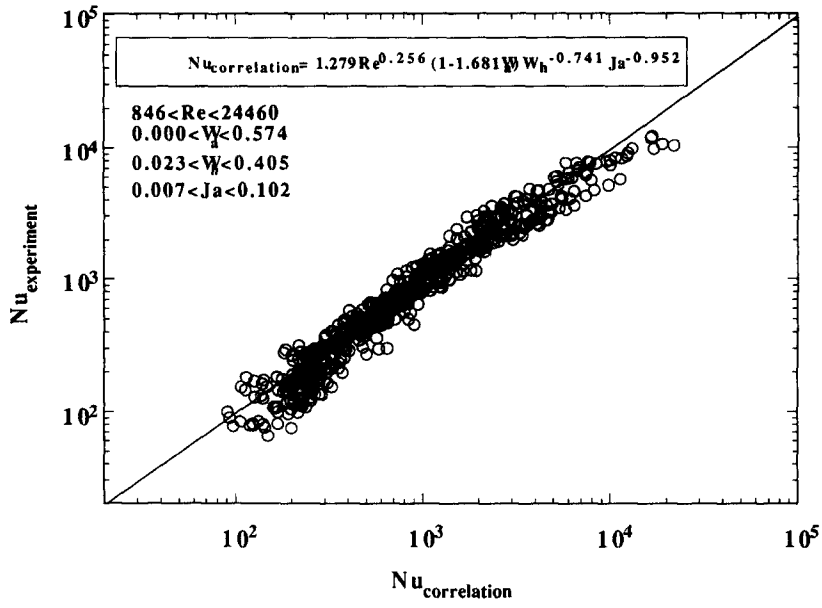

Fig. 8. Comparison between the experimentally obtained Nusselt numbers and those obtained by steam/air/helium correlation, equation (22).

are constant and equal to their values at the inlet of the condensing tube, the local steam flow rate $m_v^{(\kappa+1)}$, and the condensate flow rate $dm_{con}^{(\kappa+1)}$ between the node (κ) and the node $(\kappa+1)$ are given by

$$m_v^{(\kappa+1)} = m_{nc}\frac{1-W_{nc,b}^{(\kappa+1)}}{W_{nc,b}^{(\kappa+1)}} \tag{25}$$

and

$$dm_{con}^{(\kappa+1)} = m_v^{(\kappa)} - m_v^{(\kappa+1)} \tag{26}$$

where

$$W_{nc} = W_a + W_h. \tag{27}$$

(3) Assuming a value to the wall temperature $T_w^{(\kappa+1)}$, the mixture properties can be evaluated at the corresponding bulk temperature. Once the mixture properties are known, the mixture Reynolds, Schmidt and Jakob numbers can be calculated. The local wall heat flux is then obtained from

$$q_w'' = h(T_b - T_w) \tag{28}$$

where h is the local condensation heat transfer coefficient and is obtained using one of the correlations developed in the study reported here.

(4) Assuming a linear profile of the wall heat flux along $\Delta l^{(\kappa)}$ of the condensing tube length, for steady-state conditions, the total heat transfer for the κ-node $\Delta q^{(\kappa)}$ can be related to the local heat fluxes at the condenser wall $q_w''^{(\kappa)}$ and $q_w''^{(\kappa+1)}$ as follows:

$$\Delta q^{(\kappa)} = \pi d[\tfrac{1}{2}(q_w''^{(\kappa)} + q_w''^{(\kappa+1)})]\Delta l^{(\kappa)} \tag{29}$$

for $2\delta/d \ll 1$, where $\Delta q^{(\kappa)}$ is given by

$$\Delta q^{(\kappa)} = dm_{con}^{(\kappa+1)} h_{jg}^{(\kappa)} + m_{mix}^{(\kappa+1)} C_{p,mix}\Delta T_b, \tag{30}$$

and the mixture mass flow rate $m_{mix}^{(\kappa+1)}$ is given by

$$m_{mix}^{(\kappa+1)} = m_v^{(\kappa+1)} + m_{nc}. \tag{31}$$

Step 4 yields a value for $\Delta l^{(\kappa)}$. The tube length $l^{(\kappa+1)}$ at the end of the κ-node can be expressed as

$$l^{(\kappa+1)} = \sum_{\kappa=1}^{\kappa} \Delta l^{(\kappa)}. \tag{32}$$

(5) From the given wall temperature profile, the tube length $l^{(\kappa+1)}$ is used to calculate $T_w^{(\kappa+1)}$. If this is different than the guessed value in step 3, a new value is assumed and the steps from 3–5 are repeated until a consistent solution is reached.

(6) A new bulk temperature step ΔT_b down the condenser tube length is taken and the calculation from step 1 to step 5 is repeated. The calculation is terminated when the steam in the mixture is depleted or when the end of a known condensing tube length is reached, i.e. when $l^{(\kappa+1)} \geqslant l_o$, where l_o is the effective length of the condensing tube.

5. THEORETICAL MODEL

The condensate film will be dealt with first. An appropriate correlation for condensate film heat transfer coefficient is to be selected. Given the local wall temperatures T_w, the local values of the mixture/condensate interface temperature T_i can then be calculated along the condensing tube length. Next, the steam/noncondensable gas mixture will be modeled. The heat transfer coefficients of steam/gas mixture,

obtained using the model, will then be compared to those obtained from the experimental measurement.

5.1. *Condensate film*

The condensate film will be modeled as an annular layer on the inside of the vertical condensing tube. Chen *et al.* [28] developed a general in-tube condensation correlation which incorporates the effects of interfacial shear stress, interfacial waviness and turbulent transport in the condensate film. This correlation is established on the basis of analytical and empirical results from the literature and is found to be in excellent agreement with all existing data [28]. For local condensation Nusselt numbers for concurrent annular-film flow inside a vertical tube, the correlation is expressed in equations (6) and (7). Once the local condensate film Nusselt number is known, the local condensate film heat transfer coefficient h_f (kW m^{-2} s^{-1}) and the local condensate film thickness δ_f (m) can be obtained from the following expressions:

$$h_f = \frac{k_f}{\left(\frac{v_f^2}{g}\right)^{1/3}} Nu_f \tag{33}$$

and

$$\delta_f = \frac{\left(\frac{v_f^2}{g}\right)^{1/3}}{Nu_f} \tag{34}$$

where the local condensate film Reynolds number Re_f is given by equation (4) for

$$\frac{2\delta_f}{d} \ll 1.$$

The condensate film properties are evaluated at a reference temperature $T_r = T_w + 0.33(T_i - T_w)$ where T_i is the interface temperature and T_w is the condensing tube inner wall temperature. The local condensate film flow rate m_{con} can be calculated from the experimental measurement as described in equation (3). An initial guess for the interface temperature is assumed and equations (4), (6), (7) and (33) can be used in this order to obtain the local condensate film heat transfer coefficient h_f. Once h_f is known, the interface temperature T_i is calculated from

$$T_i = T_w + \frac{q''}{h_f} \tag{35}$$

where q'' is the local heat flux obtained from the experimental measurements, equation (1). The new interface temperature is then used together with the system of equations (4), (6), (7) and (33) to improve the initial guess. This is repeated until a consistent solution is reached.

Figure 9 shows the measured bulk, measured wall, and the calculated interface temperature profiles for a typical experimental run. The mixture Reynolds numbers are relatively low and cover the range from about 1000 to 4000. The flow is believed to be laminar for mixture Reynolds numbers less than 2300 and turbulent for mixture Reynolds number greater than 2300. The mixture Reynolds number profile is also shown in the figure. The interface temperatures are calculated following the procedure outlined above. The calculated interface profile is very close to the wall temperature profile and eventually converges into it near the end of the condensing tube as the mixture Reynolds numbers get well into the laminar flow region. This shows that, at these relatively low mixture Reynolds numbers the thermal resistance due to the condensate film is a small fraction of the total thermal resistance and almost negligible as the mixture flow becomes laminar. In other words, at relatively low mixture Reynolds numbers, the main thermal resistance comes from the steam/noncondensables mixture and in practice the interface temperature may be assumed to be equal with the wall temperature without introducing any significant error.

Figure 10 shows the measured bulk, measured wall and the calculated interface temperature profiles for another experimental run. The mixture Reynolds numbers are relatively high and cover the range from about 6000 to 17000. The mixture flow is definitely turbulent. The mixture Reynolds number profile is also shown in the figure. The calculated interface temperature profile starts almost halfway in between the bulk temperature profile and the wall temperature profile, which means that the condensate film thermal resistance is comparable to the mixture thermal resistance. As the mixture flows down, the interface temperature profile parallels the wall temperature profile while it diverges from the bulk temperature profile. This behavior is due to two reasons. First, as the mixture flows down the condensing tube, the mixture becomes less turbulent, and second it gets richer in noncondensable gas content. Both mechanisms contribute to the mixture thermal resistance increase. This shows that, in forced convection flows, at high mixture Reynolds numbers the thermal resistance due to the condensate film is comparable to the mixture thermal resistance at relatively low noncondensable mass fraction ($W_{nc} < 0.2$), and it gets smaller as the noncondensable mass fraction increases. Under those conditions, the thermal resistance due to the condensate film is important, and the assumption of equal interface temperature and wall temperature would introduce significant error.

5.2. *Steam-noncondensable boundary layer*

The steady-state diffusion equation in the radial direction y of each component in the mixture can be written as

$$m_v'' = -\rho D \frac{\partial W_v}{\partial y} + W_v m_v'' \tag{36}$$

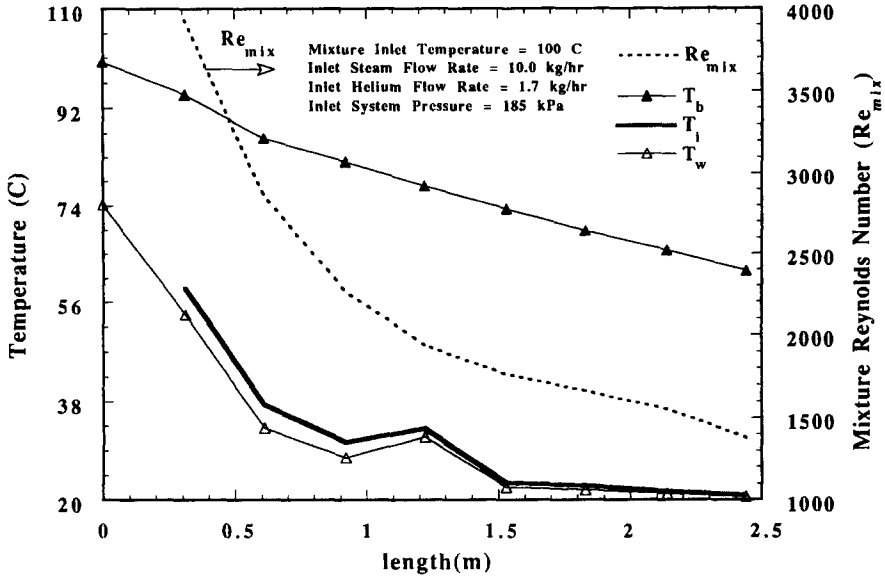

Fig. 9. The calculated interface temperatures, the measured centerline and inner wall temperatures along the condensing tube length for a typical steam–helium run in forced convection flow.

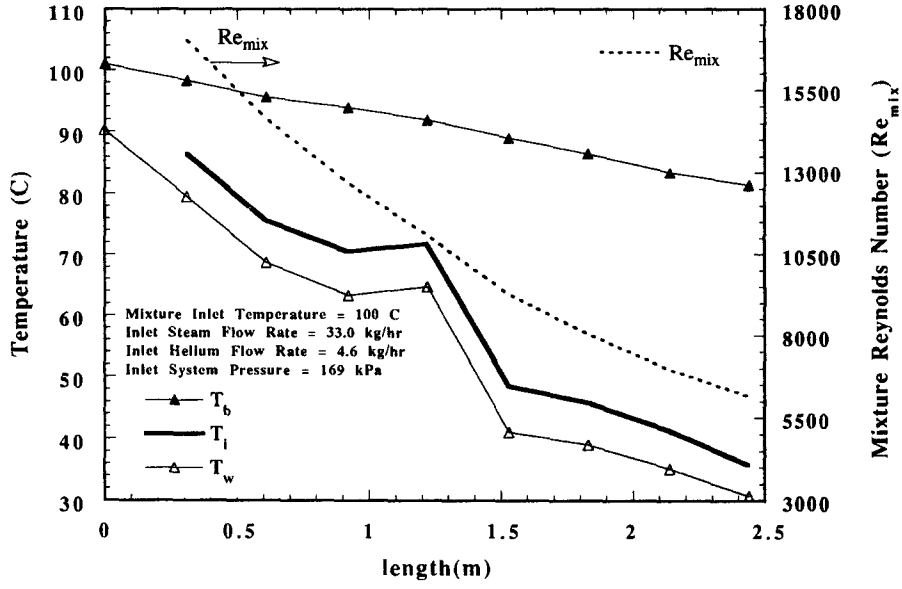

Fig. 10. The calculated interface temperatures, the measured centerline and inner wall temperatures along the condensing tube length for a typical steam–helium run in turbulent forced convection flow.

$$m''_a = -\rho D_a \frac{\partial W_a}{\partial y} + W_a m''_t, \tag{37}$$

$$m''_h = -\rho D_h \frac{\partial W_h}{\partial y} + W_h m''_t \tag{38}$$

and

$$m''_t = m''_v + m''_a + m''_h \tag{39}$$

where m''_v, m''_a, m''_h, and m''_t are the steam diffusive mass flux, air diffusive mass flux, helium diffusion mass flux, and total diffusive mass flux, respectively. W_v, W_a and W_h are the steam mass fraction, air mass fraction and helium mass fraction, respectively. ρ is the mixture density. D_v, D_a, and D_h are the effective mass diffusivities for steam, air and helium, respectively.

In the problem at hand, while the steam condenses at the inner wall of the condensing tube, the air and helium do not. In other words, the condensate interface is impermeable to both air and helium. Therefore, the net diffusive air and helium fluxes should be zero. This is expressed mathematically as

$$m''_a = m''_h = 0 \quad \text{and} \quad m''_t = m''_v = \text{const.} \tag{40}$$

along the y-direction and equations (39)–(41) are reduced to

$$m''_v = -\rho D \frac{\partial W_v}{\partial y} + W_v m''_v \tag{41}$$

$$0 = -\rho D\frac{\partial W_a}{\partial y} + W_a m''_v \tag{42}$$

$$0 = -\rho D\frac{\partial W_h}{\partial y} + W_h m''_v. \tag{43}$$

Therefore, the transport phenomenon within the gaseous boundary layer can be viewed as unidirectional diffusion, only one molecular species—that of vapor—diffuses through helium and air which are motionless in the radial direction relative to stationary coordinates. D in the above equations is equal to D_v which is given by [31]

$$D_v = \left(\frac{Y^v_a}{D_{va}} + \frac{Y^v_h}{D_{vh}}\right)^{-1} \tag{44}$$

where Y^v refers to the mole fraction compositions on a vapor-free basis. D_{va} and D_{vh} are the binary diffusion coefficients between vapor and air, and vapor and helium, respectively, and are obtained from the following equation [12]:

$$D_{12} = \frac{6.6\times 10^{-4}T^{1.83}}{P\left[\left(\frac{T_c}{P_c}\right)_1^{1/3} + \left(\frac{T_c}{P_c}\right)_2^{1/3}\right]^3}\sqrt{\frac{1}{M_1}+\frac{1}{M_2}} \tag{45}$$

where 1 refers to one component in the binary mixture, while 2 refers to the other component. T_c (°K) refers to the critical temperature and P_c (kPa) refers to its corresponding critical pressure.

Steam/noncondensables boundary layer thermal equilibrium condition. The basic assumption in the present analysis of the steam/noncondensables boundary layer is that the components of the steam/air/helium mixture are in thermal equilibrium with one another. Another assumption is that the steam within the mixture is, and remains, saturated over the entire length of the condensing tube. The mixture temperature at any location within the steam/noncondensable boundary layer is therefore equal to the saturation temperature corresponding to the vapor pressure at this location, i.e.

$$T_a = T_h = T_v = T \quad T_v = T_{sat}\{P_v\}. \tag{46}$$

Alternatively;

$$P_v = P_{sat}\{T\}. \tag{47}$$

The third assumption is that each of the gases in the mixture obeys the perfect gas law and consequently Gibbs–Dalton perfect gases mixture equation, i.e.

$$W_v = \frac{M}{M_v}\frac{P_v}{P_t} \tag{48}$$

where M_v is the vapor molecular weight, P_t is the system total pressure, and M is the mixture molecular weight given by

$$\frac{1}{M} = \frac{W_v}{M_v} + \frac{W_a}{M_a} + \frac{W_h}{M_h}. \tag{49}$$

From the conservation of mass

$$W_v + W_a + W_h = 1. \tag{50}$$

Also, over the entire length of the condenser, the air flow rate and the helium flow rate remain the same and are equal to their values at the inlet. This leads to their ratio at any location be the same and given by

$$\frac{W_h}{W_a} = \frac{W_h^{in}}{W_a^{in}} = \text{const.} \tag{51}$$

where W_a^{in} and W_h^{in} are the inlet air mass fraction and the inlet helium mass fraction, respectively.

Steam mass flux m''_v *at the interface.* With the assumption that the mixture density ρ and the effective diffusivity D are not a function of the radial position y (they will be evaluated at a reference temperature and a reference composition as shown in ref. [25]), equations (42) and (43) can be added, rearranged and then integrated as follows:

$$\int_{W_{v,i}}^{W_{v,b}} \frac{d(1-W_v)}{(1-W_v)} = \frac{m''_v}{\rho D}\int_0^y dy \tag{52}$$

$$m''_v = \frac{\rho D}{y}\ln\left(\frac{1-W_{v,i}}{1-W_{v,b}}\right). \tag{53}$$

By definition

$$W_{nc,i} = 1 - W_{v,i} \quad \text{and} \quad W_{nc,b} = 1 - W_{v,b} \tag{54}$$

and therefore

$$W_{nc,i} - W_{nc,b} = W_{v,b} - W_{v,i}. \tag{55}$$

Using equations (54) and (55), equation (53) can be written as

$$m''_v = \frac{\rho D}{y}\frac{W_{v,b}-W_{v,i}}{W_{nc,i}-W_{nc,b}}\ln\left(\frac{W_{nc,i}}{W_{nc,b}}\right). \tag{56}$$

Now define W_{nc}^{lm} such that

$$W_{nc}^{lm} = \frac{W_{nc,i}-W_{nc,b}}{\ln\left(\frac{W_{nc,i}}{W_{nc,b}}\right)} \tag{57}$$

is the logarithmic mean difference between the noncondensable gas concentrations in the bulk and at the interface. Equation (56) can then be rewritten as

$$m''_v = \frac{\rho D}{y W_{nc}^{lm}}(W_{v,b} - W_{v,i}). \tag{58}$$

The noncondensable gases do not diffuse. However, their concentration gradients are established by friction with vapor molecules as they move towards the condensate/gaseous boundary layer interface. This intermolecular friction is the source of the noncondensables inhibiting effect on the condensation process. This inhibiting effect can be well represented

by the average noncondensables concentration W_{nc}^{lm} which appears in equation (58).

Effect of axial flow: effective mixture boundary layer thickness δ_{eff}. So far, the effect of axial flow has not been considered in the above analysis. The distance y from the interface in equation (58) is the parameter which carries this effect and is going to be replaced by the symbol δ_{eff} from now on. This effective thickness is very similar in concept to the boundary layer thickness. The higher the axial flow, the thinner this effective thickness is, and consequently the higher the mass transfer m_v''. This is also what has been observed in practice; the higher the mixture Reynolds number, the higher the condensation rate. As the mixture flows along the condensing tube, vapor is continuously sucked toward the wall. In the absence of this suction, the mixture boundary layer would develop until it becomes fully developed at a certain axial location depending on the mixture Reynolds number at the entrance. However, within the condensation region, the mixture boundary layer will not have the chance to fully develop and the mixture boundary layer thickness is expected to be much thinner than that without condensation. Therefore, we will assume relationships between the mixture boundary layer δ_{eff} and the mixture Reynolds number Re_{mix} which will take the form

$$\frac{\delta_{eff}}{d} = \frac{C}{Re_{mix}^{n} Sc_{mix}^{m}} \tag{59}$$

where C, n and m are constants to be determined. In the present analysis we use, for laminar flows, $C = 5$, $n = 1/2$ and $m = 1/3$, while for turbulent flows, $C = 0.17$, $n = 1/5$ and $m = 0$, with the dependence on mixture Schmidt number dropped. The values of these constants are close to those used for developing flows.

Local interfacial heat flux $q''_{mix,i}$ *and mixture Nusselt number* Nu_{mix}. Within the condensation length, the local heat fluxes are practically due to the latent heat given by the steam at the wall. The sensible heat from the mixture due to the temperature differential in the radial direction can be practically neglected. Therefore, the local heat flux $q''_{mix,i}$ can be simply obtained by multiplying both sides of equation (58) by h_{fg} with y replaced by δ_{eff}, i.e.

$$q''_{mix,i} = m''_v h_{fg} = \frac{\rho D}{\delta_{eff} W_{nc}^{lm}} (W_{v,b} - W_{v,i}). \tag{60}$$

Define the mixture heat transfer coefficient h_{mix} and the mixture Nusselt number as

$$h_{mix} = \frac{q''_{mix,i}}{T_b - T_i} \tag{61}$$

$$Nu_{mix} = \frac{h_{mix} \times d}{k} \tag{62}$$

where k is the mixture thermal conductivity. The mixture Nusselt number is therefore;

$$Nu_{mix} = \frac{Pr_{mix}}{Ja_{mix} Sc_{mix}} \frac{d}{\delta_{eff}} \frac{1}{W_{nc}^{lm}} (W_{v,b} - W_{v,i}). \tag{63}$$

Substituting for δ_{eff} from equation (59) into equation (63), a final expression for the mixture Nusselt number Nu_{mix} is obtained. It is given by

$$Nu_{mix} = \frac{Pr_{mix}}{Ja_{mix}} \frac{Re_{mix}^{n} Sc_{mix}^{n-1}}{C W_{nc}^{lm}} (W_{v,b} - W_{v,i}) \tag{64}$$

where Pr_{mix}, Ja_{mix} and Sc_{mix} are mixture Prandtl, Jakob and Schmidt numbers, respectively. An explicit expression for the mixture heat transfer coefficient can be obtained from the definition

$$h_{mix} = \frac{k}{d} \times Nu_{mix} \tag{65}$$

where Nu_{mix} in the above equation is obtained from equation (64).

All mixture properties in the above equations are evaluated at a reference composition and temperature using the procedure outlined in ref. [25].

Now, let us turn to the comparison between the mixture heat transfer coefficients as obtained from experimental measurement and those obtained from the model presented here, namely equations (64) and (65). The measured Nusselt number and heat transfer coefficient are obtained from

$$h_{mix,exp} = \frac{q''_{exp}}{T_b - T_i}, \tag{66}$$

$$Nu_{mix,exp} = \frac{h_{mix,exp} \times d}{k} \tag{67}$$

where T_i is the interface temperature calculated using the procedure outlined in Section 5.1 and q''_{exp} is the measured wall heat flux at the inner wall of the condensing tube and is obtained using the gradient of the coolant temperature profile. This measured value of q''_{exp} is practically equal to the heat flux at the interface, since the condensate film thickness δ is much less than the condensing tube inner diameter d so that $d/(d-2\delta) \approx 1$. Figure 11 shows the measured and the calculated mixture heat transfer coefficient profiles for a typical experimental run. The mixture Reynolds number profile is also shown in this figure. In general, the mixture heat transfer coefficients obtained using the model are in good agreement with the measured mixture heat transfer coefficients. Figure 12 shows a comparison between the model-predicted steam/noncondensables mixture Nusselt numbers as calculated from equation (64) and the experimentally obtained Nusselt numbers. Again, the figure shows good agreement between the model and the experiment with the values of n, m and C in equation (64) taken equal to 0.2, 0.0, and 0.185, respectively, for turbulent flows, while for laminar flows the n, m and C values taken equal to 0.5, 1/3 and 5, respectively. Figure 12 shows that below a Nusselt number of 100 (corresponding mainly to laminar flows) the scattering

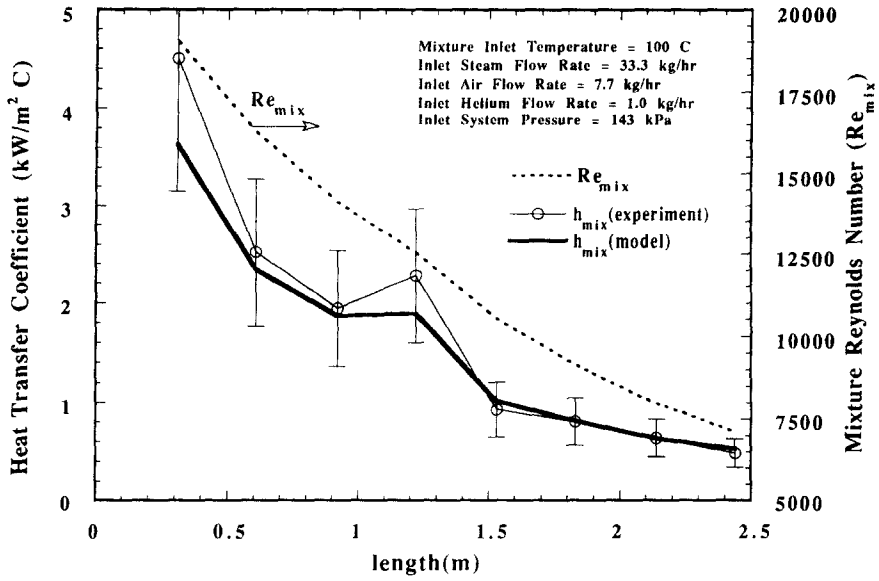

Fig. 11. The calculated mixture heat transfer coefficients (HTCs) and the measured HTCs for a typical steam–air–helium run in forced convection flows.

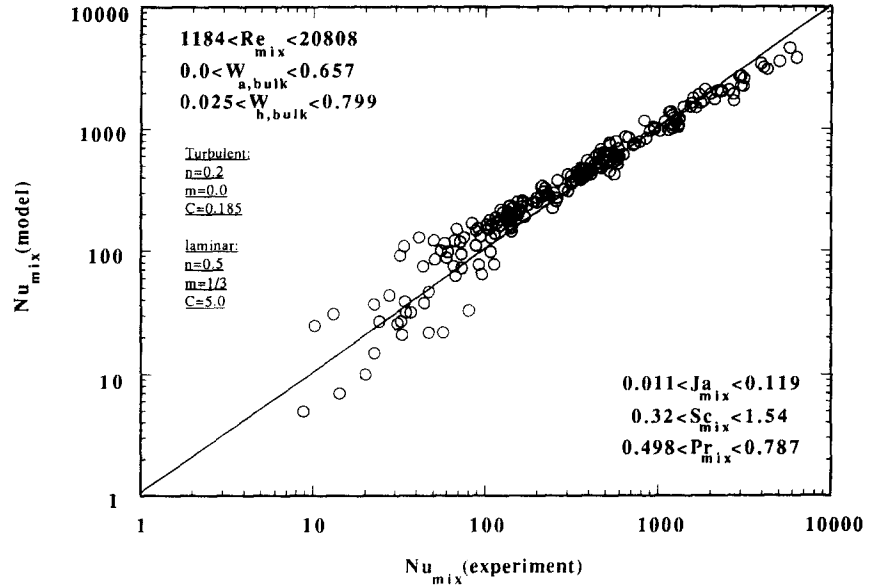

Fig. 12. Comparison between model-predicted steam/noncondensable mixture Nusselt numbers and experimentally obtained mixture Nusselt numbers.

is relatively high between the model-predicted values and the experimentally obtained ones.

6. CONCLUSIONS

The condensation of flowing steam/helium and steam/air/helium mixtures has been experimentally investigated over a wide range of system parameters. The experimentally obtained local condensation heat transfer coefficients were correlated in terms of the controlling parameters. The developed correlations predict the experimental data very well, and can be used in order to predict the local condensation heat transfer coefficients inside vertical tubes for the range of conditions utilized in the experiments reported in this study. Correlations including the mixture Schmidt number did better in representing the condensation process in the presence of noncondensable gases. The Siddique–Golay–Kazimi's steam/helium correlation prediction of the condensation heat transfer coefficients was found to be in reasonable agreement with the steam/helium experimental condensation heat transfer coefficients reported here. In general, the condensate film thermal resistance is significant in forced convection in-tube condensation in the presence of noncondensable gases, when the gas mixture

Reynolds number are high ($Re > 6000$) and the mass fraction of the noncondensable gases of the mixture is low ($W < 0.2$). The theoretical model presented here seems to reasonably predict the experimentally obtained heat transfer coefficients.

REFERENCES

1. K. M. Jensen, Condensation with noncondensables and in multicomponent mixtures. In *Two Phase Flow Heat Exchangers* (Edited by S. Kadac, A. E. Bergles and E. O. Fernandes), pp. 293–324. Kluwer Academic, Dordrecht (1988).
2. M. K. Vierow, Behavior of steam-air systems condensing in concurrent vertical down flow, MS thesis, Nuclear Engineering, University of California at Berkeley, Berkeley, CA (1990).
3. A. A. Dehbi, M. W. Golay and M. S. Kazimi, The effects of noncondensable gases on steam condensation under turbulent natural conditions, MIT-ANP-TR-004, Department of Nuclear Engineering, Massachusetts Institute of Technology, Cambridge, MA (1991).
4. G. D. Ogg, Vertical down flow condensation heat transfer in gas–steam mixtures, MS Thesis, Nuclear Engineering, University of California at Berkeley, Berkeley, CA (1991).
5. M. Siddique, M. W. Golay and M. S. Kazimi, The effect of noncondensable gases on steam condensations under forced convection conditions, MIT-TR-010, Department of Nuclear Engineering, Massachusetts Institute of Technology, Cambridge, MA (1992).
6. M. L. Corradini, Turbulent condensation on a cold wall in the presence of noncondensable gas, *Nuclear Technol.* **64,** 186–195 (1984).
7. J. C. Y. Koh, Two-phase boundary layer in laminar film condensation, *Int. J. Heat Mass Transfer* **2,** 69–82 (1969).
8. J. W. Rose, Condensation of a vapor in the presence of a noncondensable gas, *Int. J. Heat Mass Transfer* **12,** 223–237 (1969).
9. W. J. Minkowycz and E. M. Sparrow, Condensation heat transfer in the presence of noncondensables, interfacial resistance, superheating, variable properties and diffusion, *Int. J. Heat Mass Transfer* **9,** 1125–1144 (1966).
10. E. M. Sparrow, W. J. Minkowycz and M. Saddy, Forced condensation in the presence of noncondensables and interfacial resistance, *Int. J. Heat Mass Transfer* **10,** 1829–1845 (1967).
11. V. E. Denny, A. F. Mills and V. J. Jusionis, Laminar film condensation from a steam–air mixture undergoing forced flow down a vertical surface, *J. Heat Transfer* **93,** 297–304 (1971).
12. T. Fujii, *Theory of Laminar Film Condensation.* Springer, Berlin (1991).
13. J. W. Rose, Approximate equations for forced convection condensation in the presence of a noncondensing gas on a flat plate and a horizontal tube, *Int. J. Heat Mass Transfer* **23,** 539–546 (1980).
14. A. C. Bannwart and A. Bontemps, Condensation of a vapour with incondensables; an improved gas film model accounting for the effect of mass transfer on film thicknesses, *Int. J. Heat Mass Transfer* **33,** 1465–1474 (1990).
15. P. Kaiping and U. Renz, Thermal diffusion effects in turbulent partial condensation, *Int. J. Heat Mass Transfer* **34,** 2629–2639 (1991).
16. A. P. Colburn and O. A. Hougen, Design of cooler condensers for mixtures of vapors with noncondensing gases, *Ind. Engng Chem.* **26,** 1178–1182 (1934).
17. J. F. Votta and C. A. Walker, Condensation of vapor in the presence of noncondensing gas, *A.I.Ch.E. J.* **4,** 413–417 (1958).
18. C. K. Nithianandan, C. D. Morgan and N. H. Shah, RELAP5/MOD 2 model for surface condensation in the presence of noncondensable gases, *Proceedings of the Eighth International Heat Transfer Conference*, Vol. 4, pp. 1627–1633 (1986).
19. M. H. Kim and M. L. Corradini, Modeling of condensation heat transfer in a reactor containment, *Nuclear Engng Des.* **118,** 193–212 (1990).
20. M. Siddique, M. W. Golay and M. S. Kazimi, Local heat transfer coefficients for forced convection condensation of steam in a vertical tube in the presence of air, *Two-Phase Flow and Heat Transfer*, HTD-Vol. 197. ASME, New York (1992).
21. P. F. Peterson, V. E. Schrock and T. Kageyama, Diffusion layer theory for turbulent vapor condensation with noncondensable gases, *ASME/ANS National Heat Transfer Conference*, San Diego (1992).
22. K. Asano, Y. Nakano and M. Inabe, Forced convection film condensation of vapor in the presence of noncondensable gas on a small vertical plate, *J. Chem. Engng Jap.* **12,** 196–202 (1979).
23. W. H. McAdams, *Heat Transmission* (3rd Edn), pp. 223–319. McGraw-Hill, New York (1975).
24. H. A. Hasanein, M. W. Golay and M. A. Kazimi, The effect of cooling conditions on in-tube condensation in the presence of noncondensables, *Ninth Proceedings of Nuclear Thermal Hydraulics*, pp. 140–147 (1993).
25. H. A. Hasanein, M. W. Golay and M. S. Kazimi, Steam condensation in the presence of noncondensable gases under forced convection conditions, MIT-ANP-TR-024, Department of Nuclear Engineering, Massachusetts Institute of Technology, Cambridge, MA, July (1994).
26. W. Nusselt, Die Oberflachenkondensation des Wasserdampfes, *Z. Ver. Deut. Ing.* **60,** 541–546 (1916).
27. J. G. Collier, *Convective Boiling and Condensation.* McGraw-Hill, New York (1972).
28. S. L. Chen, F. M. Germer and C. L. Tien, General film condensation correlation, *Expl. Heat Transfer* **1,** 93–107 (1987).
29. F. T. Irvine and P. E. Liley, *Steam and Gas Tables with Computer Equations.* Academic Press, Ontario (1984).
30. R. C. Reid, M. Prausnitz and T. K. Sherwood, *The properties of Gases and Liquids* (3rd Edn). McGraw-Hill, New York (1977).
31. R. E. Treybal, *Mass Transfer Operation.* McGraw-Hill, New York (1955).